24th International Conference on Renewable Energies and Power Quality (ICREPQ'26)
Santander (Spain), 10th to 12th June 2026
ISBN-13: 978-84-09-82044-3

Automated Time-Domain Detection and Characterization of Supraharmonic Impulsive Emissions

I. Zuazo[1], A. Gallarreta[1,*], J. González-Ramos[1], J. Vildósola[1], I. Angulo[1], I. Fernández[1], A. Arrinda[1], D. de la Vega[1]

[1]University of the Basque Country (UPV/EHU)
48013 Bilbao (Spain)
[*]Phone number: +34 946017381, e-mail: alexander.gallarreta@ehu.eus

Abstract. Power-electronics-based devices inject conducted impulsive disturbances into low-voltage grids, which can interfere with grid operation, connected devices, and power line communications. This work presents a methodology for the automated measurement and characterization of unwanted high-amplitude impulsive disturbances. First, the paper proposes a set of algorithms for the automatic acquisition of voltage measurements of conducted emissions. The algorithms controls a commercial oscilloscope, processes the raw voltage data, detects high-amplitude impulsive disturbances, and stores those sporadic emissions to optimize storage resources. These algorithms provide high reliability and a modular architecture to enable the integration of additional analytical functionalities. The second step of the methodology involves the automatic characterization of the stored impulsive waveforms, by delimiting the waveform, extracting its main features with a set of representative parameters, and applying a search algorithm to detect similar waveforms. The search algorithm relies on cross-correlation to identify similarities and performs a statistical analysis to quantify variability. In addition, the statistical analysis assesses a benchmark-waveform and extracts the temporal and magnitude features. The paper presents results of some impulsive waveforms to demonstrate the effectiveness of the proposed methodology.

Key words. Electromagnetic compatibility, power-quality, supraharmonic disturbances.

1. Introduction

The high penetration of inverter- and rectifier-based devices in low-voltage (LV) distribution grids has led to a significant increase in non-intentional emissions [1],[2]. It is known that these conducted emissions can provoke unwanted effects on grid operation and on the devices connected to the grid, such as thermal stress, malfunction, and audible noise [3]-[5]. Moreover, conducted emissions interfere with power line communication (PLC) transmissions, since these disturbances are unintentionally injected into the same frequency band where PLC technologies operate [6]-[8]. Among the existing conducted emissions, impulsive disturbances are a particular type that requires specific attention and systematic analysis [9].

These impulsive emissions may be difficult to detect, because they occur only sporadically or under specific conditions [9], for example, when devices turn on or when a high-charging event starts. Moreover, they include fast magnitude variations in a very short time. For these reasons, conventional measurement devices, especially instruments for continuous measurements, do not always detect these emissions with the required accuracy, or if they do, the measurement time must be extremely long, increasing considerably the size of the recording files.

Moreover, the extremely short duration of the impulsive emissions requires high-sampling-rate measurement equipment and real-time recording systems. In the absence of such equipment, these events are difficult to be detected and examined. Furthermore, the difficulty in detecting and parametrizing the impulsive conducted emissions is a severe hindrance for developing mitigation measures that decrease their impact on grid operation.

In order to ensure an effective detection and analysis of impulsive emissions, it is necessary to develop advanced algorithms capable of conducting high-precision measurements, real-time data collection and systematic characterization. These tools must also provide high reliability and modular architecture to enable the integration of additional analytical functionalities. Current commercial software does not meet these requirements in the 9-500 kHz range: it is often incapable of detecting impulsive emissions in real time, lacks adequate precision, and is not adaptable to emerging research needs. It is therefore necessary to develop new technological solutions that reliably measure and reflect the characteristics of the impulsive emissions and provide flexibility for future developments.

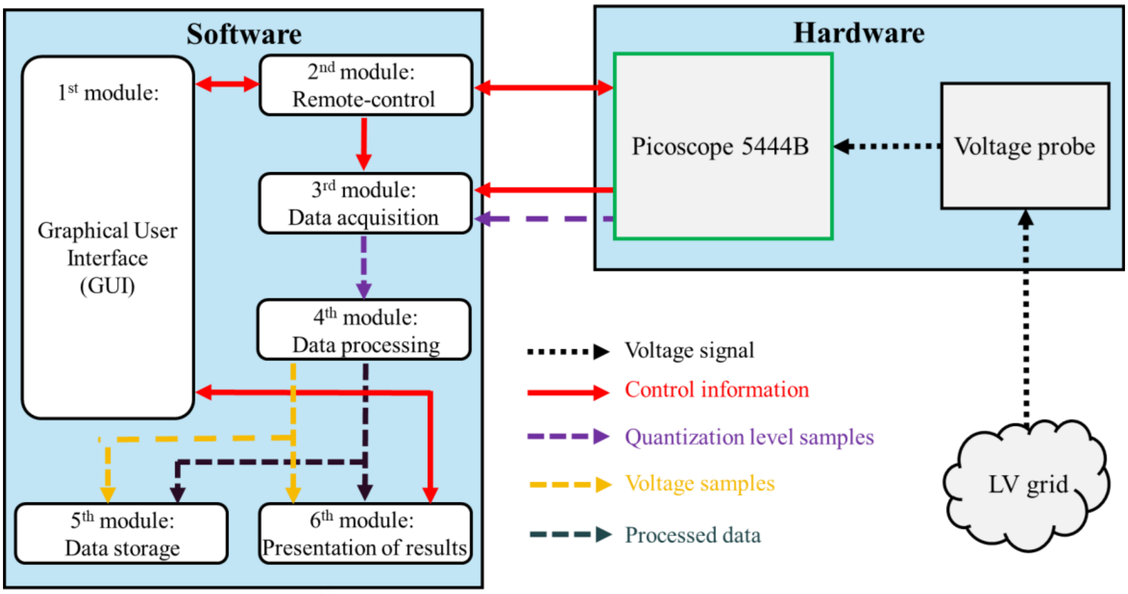

Fig. 1. Schematic overview of the proposed hardware and software measurement solution of conducted impulsive disturbances

2. Objectives

The primary objective of this work is to design and implement a specialized set of algorithms aimed at automating the measurement, alignment, and characterization of impulsive emissions propagated across LV distribution grids in the 9-500 kHz range. Within the measurement setup, an algorithm is designed to record these high-amplitude sporadic emissions with high precision and reliability. The algorithm performs measurements in real-time, utilizing a modular architecture that integrates advanced processing and statistical analysis tasks. A central feature of the proposed solution is the design and implementation of an automated detection and alignment methodology based on cross-correlation, which ensures the accurate grouping of transient events for subsequent study. Building upon this detection algorithm, a waveform-parametrization method is proposed to provide a comprehensive statistical characterization of the impulsive disturbances by extracting physical parameters and applying percentile-based analysis. This comprehensive approach not only facilitates the systematic evaluation of conducted impulsive emissions but also establishes a scalable framework capable of incorporating future measurement requirements.

3. Proposed measurement setup

The proposed solution consists of an integrated pre-designed hardware and a set of algorithms designed for the automatic and continuous measurement of conducted impulsive emissions in LV electrical grids (see Fig. 1).

The hardware architecture is built upon a custom-designed voltage probe for the 2–500 kHz frequency range. This probe includes analog filtering to remove harmonic distortions below 2 kHz, thereby concentrating amplitude resolution on lower-level components above 9 kHz, and to avoid aliasing effects above 500 kHz, and therefore, increasing the measurement accuracy. Moreover, galvanic isolation is included to enhance robustness against overvoltages and power transients and to protect the measurement equipment [10]. The voltage disturbances are acquired by this probe, and then, digitized using a PicoScope 5444B oscilloscope. The measurement instrument is controlled via an ad-hoc algorithm to overcome the limitations of standard commercial software regarding long-duration data streaming and customized sampling rates.

The measurement algorithm is structured into six interdependent modules that manage the complete data lifecycle, from acquisition to final storage (see Fig. 1). The modules are the following:

1. Graphical User Interface (GUI)
2. Remote-control
3. Data acquisition
4. Data processing
5. Data storage
6. Presentation of results

The process begins at the GUI, where the user defines operational parameters such as the sampling frequency (ranging from 1 MHz to 62.5 MHz), the dynamic range, and the detection method for impulsive disturbances. These settings are managed by the remote-control module, that establishes bidirectional communication with the oscilloscope in order to exchange control information and configuration settings. The raw data acquired by the oscilloscope is then received in the form of quantification levels by the data acquisition module. It receives continuously the acquired data in 200 ms blocks from the buffer of the oscilloscope. This modular approach allows real-time processing and data visualization without compromising the system's memory.

The core of the system is the data processing module, which converts raw digital quantification levels into voltage units and applies detection algorithms (see Fig. 1). The measurement algorithm offers two distinct operational modes for the detection of impulsive disturbances. The first detection approach relies on the amplitude: if the measured voltage samples are above an amplitude threshold, the module activates a trigger to store the data samples. The

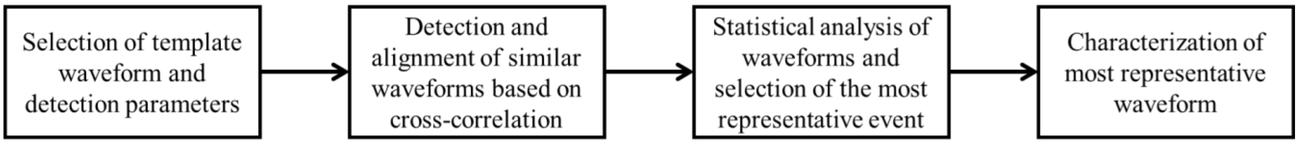

Fig. 2. Flowchart of the proposed methodology for the detection, alignment and characterization of impulsive waveforms.

amplitude threshold can be set with fixed amplitude values defined by the user, or with dynamic amplitude values based on statistics of the measured voltages (root-mean-square, median, or mean amplitude). In contrast, the second approach detects rapid amplitude changes within a time window. This approach computes the absolute amplitude changes for each sample with respect to the previous one, integrates the differences within a sliding time window, and activates a trigger if the amplitude difference exceeds a user-defined threshold within the specified time interval.

Then, when an event satisfies the detection criteria, the data storage module receives the triggers activated by the previous module, and then, the samples corresponding to the 200 ms measurement segment are automatically stored in a binary format file (see Fig. 1). Finally, all the data samples and the waveforms classified as impulsive disturbances, along with the detection thresholds, are compiled and prepared to be presented.

This structure ensures high-speed data acquisition and reduced file sizes, facilitating the subsequent analysis and the detailed characterization of impulsive phenomena in modern power grids.

4. Methodology for the characterization of impulsive disturbances

In order to characterize the impulsive disturbances automatically detected by the system, this work proposes a methodology to systematically identify, group, and parametrize waveforms of similar pattern.

The methodology is based in four steps, as indicated in Fig. 2. In the first step, an impulsive emission event is selected to be used as a “reference waveform”, being typically the first significant event detected by the measurement algorithm. In addition, a set of parameters are selected to be applied in this step to detect similar waveforms; minimum amplitude value, minimum cross-correlation output, and minimum temporal spacing between similar events. The values of this set of parameters are adjusted for each reference waveform.

The second step of the methodology aims at detecting waveforms of a similar pattern. For that, the reference waveform is used to compute the cross-correlation over all the binary files stored by the measurement system. A maximum output in the cross-correlation indicates waveform similarity; moreover, the time lag that maximizes the cross-correlation output identifies accurately the starting time of the similar waveform. This step not only detects similar waveforms but also aligns all the detected events. This automated alignment process removes effectively temporal jitter and acquisition delays, allowing for the synchronized overlay of multiple emissions. This process is fundamental for identifying similar transient events and aligning them with high temporal precision, which is a critical prerequisite for any meaningful statistical analysis.

Once the emissions are properly selected and aligned, an automated statistical analysis of the phenomena is executed in the third step of the methodology. This process computes several percentiles in order to quantify the variability of the detected impulsive waveforms (see Fig. 3 and Fig. 4). While 50th percentile (median) provides the general trend of the detected waveforms, 10th and 90th percentiles provide an essential overview of the typical behavior of the disturbances while also highlighting the extreme events occurring within the LV distribution grid. Additionally, this stage also selects the “benchmark-waveform” that shows the closest similarity to the median value of the set of the detected disturbances (see Fig. 3 and Fig. 4). This calculation relies on the cross-correlation for selecting the

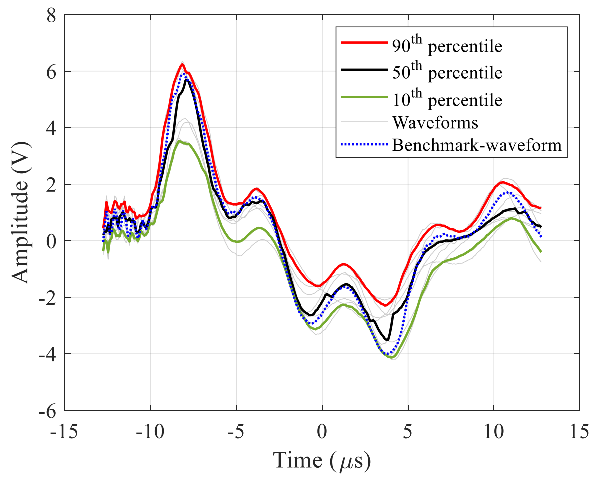

Fig. 3. First set of impulsive waveforms, the corresponding percentiles, and the automatically selected benchmark-waveform.

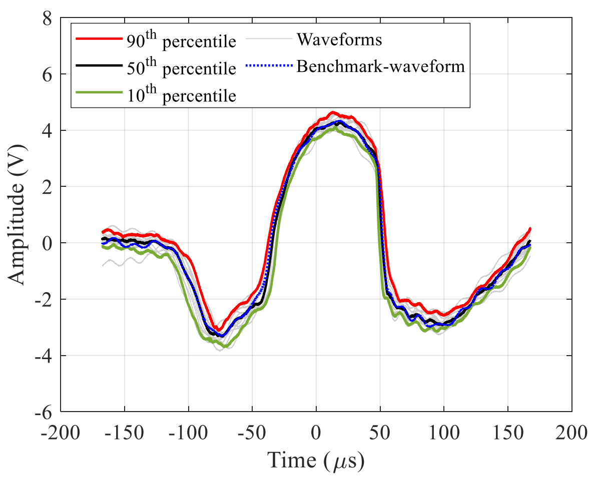

Fig. 4. Second set of impulsive waveforms, the corresponding percentiles, and the automatically selected benchmark-waveform.

waveform that provides the highest correlation value with respect to the 50th percentile values. The selected waveform will be close to the median values over the time, and therefore, it will be representative of the set of waveforms, while still being an actual measured signal rather than a synthetic statistical model. This enables the extraction of parameter values and waveform properties of the real measurements.

Lastly, the fourth step of the methodology involves the precise extraction of physical parameters of the benchmark-waveform. The chosen set of parameters to characterize the waveform provides information about the temporal behavior and the magnitude of the benchmark-waveform. For the temporal characterization, the following metrics are computed:

- Pulse duration: The total time interval of the impulsive disturbance.
- Fundamental oscillation frequency ($f_{oscillation}$): indicates the dominant frequency at which the impulsive waveform oscillates.
- Full width at half maximum (FWHM): measures the time interval between the points on the waveform at which the amplitude is half of its maximum value.
- Rise interval: determines the time interval required for the amplitude to rise from 10% to 90% of each local maximum.
- Fall interval: determines the time interval required for the amplitude to fall from 90% to 10% of each local maximum.

In order to parametrize the magnitude of the impulsive disturbances, the following metrics have been defined:

- Maximum amplitude (V_{max}): the highest voltage reached by the disturbance.
- Minimum amplitude (V_{min}): the lowest voltage reached by the disturbance under analysis.
- Peak-to-peak amplitude (V_{pp}): the total voltage range between the maximum and maximum amplitude values.
- Root-mean-square (RMS) amplitude (V_{RMS}): The quadratic mean of the waveform, representing its effective energy content.

This approach provides a robust framework for the systematic study and modelling of the time-variant behavior of impulsive disturbances in modern LV grids.

5. Results and discussion

This section presents a detailed examination of the results obtained in the parametrization and subsequent characterization of the measured emissions, following the automated processing methodology proposed in this work. The methodology described in the previous section enabled the systematic extraction of a large set of descriptors, which are synthesized here to provide a clearer understanding of the underlying waveform features. Fig. 5 and Fig. 6 give a graphical overview of several key parameters derived from the selected benchmark-waveforms (see Fig. 3 and Fig. 4). These visualizations aim not only to highlight the quantitative outcomes of the proposed analysis methodology but also to illustrate how the processing algorithms analyses the temporal and spectral structures of the captured waveforms.

Fig. 5 shows the first benchmark-waveform and presents the parametrization outcome in a graphical manner. Complementarily, Table I to Table III enumerate the most relevant characterization metrics. This waveform is a short impulsive disturbance whose duration has been delimited to 25 µs, its spectral content is dominated by an oscillation frequency of 242 kHz, and its FWHM reaches 2.59 µs, as summarized in Table I. The temporal envelope of the pulse is particularly rich in terms of rising and falling dynamics: four amplitude transitions were detected, as outlined in Fig. **3**. Their respective durations, reported in Table II, capture the variability of the transient evolution, which is relevant for classification in broader electromagnetic disturbance studies.

Magnitude-related parameters for this waveform are presented in Table III. The signal shows a maximum amplitude of 5.90 V and a minimum of -4.01 V, this is, a peak-to-peak amplitude of 9.91 V. This wide dynamic range, together with the measured RMS value of 2.28 V, confirms that the disturbance exhibits substantial energy concentration within a very short interval. Such characteristics are representative of impulsive emissions typically associated with fast-switching events or abrupt load variations, and illustrate the ability of the proposed measurement chain to capture and quantify short-duration and high-amplitude transients with high fidelity.

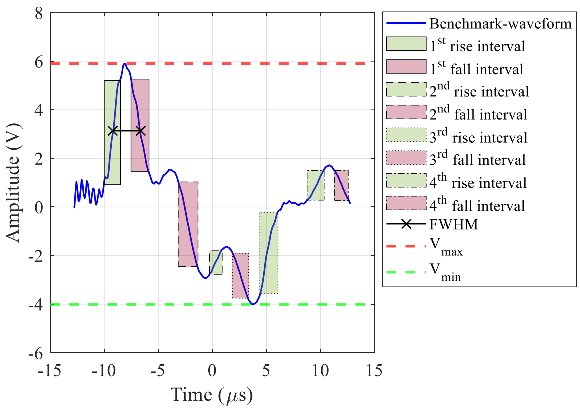

Fig. 5. First benchmark-waveform along with some of the extracted parameters.

TABLE I. TEMPORAL PARAMETERS OF THE FIRST BENCHMARK-WAVEFORM

Duration	$f_{oscillation}$	FWHM
25.38 µs	242.25 kHz	2.59 µs

TABLE II. RISE AND FALL INTERVALS OF THE FIRST BENCHMARK-WAVEFORM

	1st	2nd	3rd	4th
Rise intervals	1.50 µs	1.18 µs	1.75 µs	1.58 µs
Fall intervals	1.67 µs	1.82 µs	1.48 µs	1.27 µs

TABLE III. AMPLITUDE PARAMETERS OF THE FIRST BENCHMARK-WAVEFORM

V_{max}	V_{min}	V_{pp}	V_{RMS}
5.90 V	-4.01 V	9.91 V	2.28 V

The second benchmark-waveform, whose parametrization is illustrated in Fig. 6 shows the results for a different recording, which presents significantly different temporal and spectral properties. The results in the figure show the benchmark-waveform and the results of the parametrization. Its overall duration extends to 333 µs, much longer than the previous case. The dominant oscillation frequency is significantly lower (6.15 kHz), while the FWHM reaches 85 µs. These parameters point to a slower, more sustained disturbance whose characteristics suggest a different underlying mechanism generating the waveform. In terms of amplitude transitions, two falling intervals and one rising interval were identified, whose specific durations of these intervals are detailed in Table V.

Regarding the magnitude of this waveform, the amplitude boundaries range from 4.34 V to -3.33 V, producing a peak-to-peak amplitude of 7.67 V (see Table VI). Although lower than in the previous waveform, this value still indicates a notable fluctuation within the signal envelope. The RMS value of 2.42 V reflects a similar effective energy distribution than the previous impulsive disturbance. These parameters provide an overall and complete picture of the behavior of the waveform and demonstrate the adaptability of the set of algorithms to different emission typologies.

These results demonstrate the robustness and versatility of the automated measurement and characterization set of algorithms. It is able to effectively handle large volumes of raw data, identify and gather recursive short impulsive events, accurately extract meaningful parameters, and obtain significant information useful to identify potential sources and/or to evaluate the impact on the devices connected to the grid. The proposed algorithms and analysis methodology can be a useful and efficient tool for conducting comprehensive long-term monitoring of impulsive events in the LV distribution grid.

6. Conclusions

This work introduces a complete, automated approach for detecting, storing, and characterizing high-amplitude impulsive disturbances in LV distribution grids. By combining a novel acquisition platform with dedicated processing algorithm, the proposed system is able to capture short-duration and high-amplitude transient events that conventional measurement setups may miss. The modular algorithm architecture ensures continuous high-frequency sampling, selective storage of relevant events, and flexible adaptation to future analysis requirements.

A key contribution of the methodology is the use of cross-correlation to both identify and align similar impulsive waveforms. This automated alignment removes the timing jitter of sporadic disturbances and enables meaningful statistical comparisons across large datasets. The subsequent percentile-based analysis provides a clear picture of variability within each group of emissions, while the selection of a benchmark-waveform, which is chosen for its similarity to the median, ensures that the extracted physical parameters correspond to a real measured event rather than a purely statistical construct.

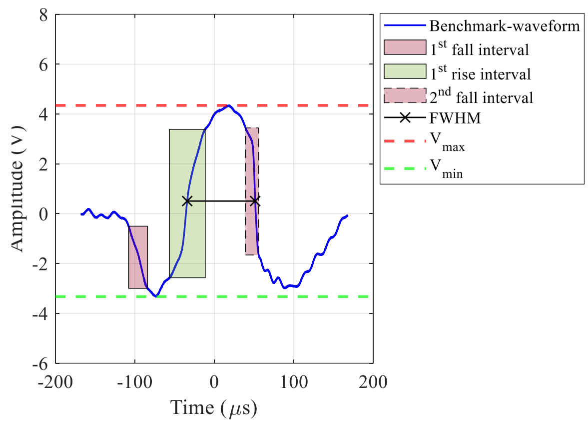

Fig. 6. Second benchmark-waveform along with some of the extracted parameters.

TABLE IV. TEMPORAL PARAMETERS OF THE SECOND BENCHMARK-WAVEFORM

Duration	$f_{oscillation}$	FWHM
333.98 µs	6.15 kHz	85.56 µs

TABLE V. RISE AND FALL INTERVALS OF THE SECOND BENCHMARK-WAVEFORM

	1st	2nd
Rise intervals	45.09 µs	
Fall intervals	23.88 µs	16.51 µs

TABLE VI. AMPLITUDE PARAMETERS OF THE SECOND BENCHMARK-WAVEFORMS

V_{max}	V_{min}	V_{pp}	V_{RMS}
4.34 V	-3.33 V	7.67 V	2.42 V

The two benchmark-waveforms presented in the paper demonstrate that the proposed methodology can detect and parametrize successfully different emission profiles: from short high-frequency pulses up to longer lower-frequency disturbances. The temporal and magnitude metrics assessed by this methodology also show that the system can capture fast magnitude variations in waveforms, which is essential for understanding the interfering mechanisms of disturbances in order to define mitigation strategies.

In conclusion, the results confirm that the developed measurement and processing set of algorithms offers a reliable framework for long-term studies of conducted impulsive disturbances in LV distribution grids. Moreover, the methodology provides valuable support for future research in power-quality assessment and electromagnetic compatibility in LV distribution grids.

Acknowledgement

The project 23NRM01 SBS-Uncert has received funding from the European Partnership on Metrology, co-financed from the European Union's Horizon Europe Research and Innovation Programme and by the Participating States. This work was financially supported in part by the Spanish Government under project SEFONIS, grant PID2025-170561OB-I00 funded by MICIU/AEI/10.13039/501100011033 and ERDF/UE. This work was funded in part by the Basque Government under the grant IT1910-26.

References

[1] A. Vinayagam, A. Aziz, P.M. Balasubramaniyam, J. Chandran, V. Veerasamy, A. Gargoom, "Harmonics assessment and mitigation in a photovoltaic integrated network", Sustainable Energy, Grids and Networks, Vol. 20, 2019, doi: 10.1016/j.segan.2019.100264.

[2] L. M. Caro, G. Ramos, K. Rauma, D. F. C. Rodriguez, D. M. Martinez, C. Rehtanz, “State of Charge Influence on the Harmonic Distortion From Electric Vehicle Charging”, IEEE Transactions on Industry Applications, Vol. 57, 2021, doi: 10.1109/TIA.2021.3057350.

[3] T. Wohlfahrt, C. Waniek, J. M. A. Myrzik, J. Meyer and P. Schegner, "Supraharmonic disturbances: Lifetime reduction of electronic mass-market equipment by the aging of electrolytic capacitors", 2018 18th International Conference on Harmonics and Quality of Power (ICHQP), Ljubljana, Slovenia, 2018, doi: 10.1109/ICHQP.2018.8378899.

[4] Ł. Michalec, P. Kostyła, Z. Leonowicz, “Supraharmonic Pollution Emitted by Nonlinear Loads in Power Networks—Ongoing Worldwide Research and Upcoming Challenges”, Energies, Vol. 16, 2023. doi: 10.3390/en16010273.

[5] A. Mariscotti, A. Mingotti, “The Effects of Supraharmonic Distortion in MV and LV AC Grids”, Sensors, Vol. 24, 2024, doi: 10.3390/s24082465

[6] M. Wasowski et al., "Sources of Non-Intentional Supraharmonics in LV Network and Its Impact on OSGP PLC Communication – Experimental Study," IEEE Transactions on Power Delivery, Vol. 37, 2022, doi: 10.1109/TPWRD.2022.3175090.

[7] D. Shrestha, X. Mestre, M. Payaró, "On channel estimation for power line communication systems in the presence of impulsive noise", Computers & Electrical Engineering, Vol. 72, 2018, doi: 10.1016/j.compeleceng.2018.10.006.

[8] I. Elfeki, S. Jacques, I. Aouichak, T. Doligez, Y. Raingeaud, J.-C. Le Bunetel, “Characterization of Narrowband Noise and Channel Capacity for Powerline Communication in France”, Energies. Vol. 11, 2018, doi: 10.3390/en11113022.

[9] S.K. Rönnberg, M.H.J. Bollen, H. Amaris, G.W. Chang, I.Y.H. Gu, Ł.H. Kocewiak, J. Meyer, M. Olofsson, P.F. Ribeiro, J. Desmet, “On waveform distortion in the frequency range of 2 kHz–150 kHz—Review and research challenges”, Electric Power Systems Research. Vol. 150, 2017, doi: 10.1016/j.epsr.2017.04.032.

[10] I. Fernández, M. Alberro, J. Montalbán, A. Arrinda, I. Angulo, D. de la Vega, “A new voltage probe with improved performance at the 10 kHz–500 kHz frequency range for field measurements in LV networks”, Measurement, Vol. 145, 2019, doi: 10.1016/j.measurement.2019.05.106